INFECTION AND IMMUNITY, Dec. 2002, p. 7022–7032 Vol. 70, No. 12
0019-9567/02/$04.00+0 DOI: 10.1128/IAI.70.12.7022–7032.2002

Pathological and Therapeutic Significance of Cellular Invasion by *Proteus mirabilis* in an Enterocystoplasty Infection Stone Model

Rejiv B. Mathoera,[1,2]* Dik J. Kok,[1] Cees M. Verduin,[2] and Rien J. M. Nijman[3]

Subdivision of Pediatric Urology, Department of Urology,[1] and Subdivision of Pediatric Urology, Department of Urology[3] and Department of Medical Microbiology and Infectious Diseases,[2] Sophia Children's Hospital, Erasmus Medical Center, 3000 DR Rotterdam, The Netherlands

Received 11 April 2002/Returned for modification 6 June 2002/Accepted 5 August 2002

Proteus mirabilis **infection often leads to stone formation. We evaluated how bacterium-mucin adhesion, invasion, and intracellular crystal formation are related to antibiotic sensitivity and may cause frequent stone formation in enterocystoplasties. Five intestinal (Caco-2, HT29, HT29-18N2, HT29-FU, and HT29-MTX) and one ureter cell line (SV-HUC-1) were incubated in artificial urine with five *Proteus mirabilis* strains. Fluorescence-activated cell sorting (FACS), laser scanning microscopy, and electron microscopy evaluated cellular adhesion and/or invasion, pathologic changes to mitochondria, and *P. mirabilis*-mucin colocalization (MUC2 and MUC5AC). An MTT (thiazolyl blue tetrazolium bromide) assay and FACS analysis of caspase-3 evaluated the cellular response. Infected cells were incubated with antibiotics at dosages representing the expected urinary concentrations in a 10-year-old, 30-kg child to evaluate bacterial invasion and survival. All cell lines showed colocalization of *P. mirabilis* with human colonic mucin (i.e., MUC2) and human gastric mucin (i.e., MUC5AC). The correlation between membrane mucin expression and invasion was significant and opposite for SV-HUC-1 and HT29-MTX. Microscopically, invasion by *P. mirabilis* with intracellular crystal formation and mitochondrial damage was found. Double membranes surrounded bacteria in intestinal cells. Relative resistance to cotrimoxazole and augmentin was found in the presence of epithelial cells. Ciprofloxacin and gentamicin remained effective. Membrane mucin expression was correlated with relative antibiotic resistance. Cell invasion by *P. mirabilis* and mucin- and cell type-related distribution and response differences indicate bacterial tropism that affects crystal formation and mucosal presence. Bacterial invasion seems to have cell type-dependent mechanisms and prolong bacterial survival in antibiotic therapy, giving a new target for therapeutic optimalization of antibiotic treatment.**

Proteus mirabilis has been designated the most important bacterial agent in the formation of infection stones, both in normal and augmented bladders (14, 23, 26). In the period following augmentation of the bladder the pH rises and stones may be formed consisting of ammonium magnesium phosphate, calcium phosphate, and calcium apatite. This stone formation has been attributed to the rise in pH as a result of urea splitting by urease (13) or crystal formation on the bacterial capsule (9, 10). When urine pH rises crystals will form in vitro in normal human urine and in artificial urine above pH 7.3 (11, 16). For crystals to mature into calculi they also must be protected against washout from the bladder. Adhesion of crystals and/or bacteria to bladder wall cells and crystal formation inside invaded cells could be of importance. In addition, adhesion or invasion may be a target in fighting the recurring cycles of infection and stone formation. Mucins such as MUC2 and MUC5AC play a part in the interaction between crystals and cells in our cellular model and are secreted to the cellular surface (22). Their role in the incorporation of bacteria into the cell is as yet unclear. Regular irrigation of the bladder in this respect should have a beneficial effect, preventing stone formation by clearing crystals, mucus, and bacteria. However, patients undergoing clean intermittent catheterization appear to be at risk for bladder stone formation (2). Further study of the occurrence of these adhesion and invasion processes and their dependence on cell, bacterial, or crystal characteristics is warranted.

Enterocystoplasties in children are well suited for the present study. Mucus formation, bacteriuria, and stone formation in these cystoplasties are common. The cystoplasties are usually constructed to enlarge small noncompliant bladders and consist of an ileal or colonic pouch attached to the remaining bladder (9). Infecting bacteria will encounter multiple types of epithelium that differ in surface characteristics. In girls with both vaginal reconstructions and an augmented bladder, the incidence of bladder stones is especially high (23). Therefore, bacterial tropism may play a role in enterocystoplasties and differences in adhesion properties could be involved. *P. mirabilis* has been noted to invade intestinal INT407, HCT-8, Caco-2, HT-29, monkey kidney, and T24 bladder cells and several other urothelial cell lines in culture, which in some cases can be inhibited (3, 25, 32). For the invasive properties of *P. mirabilis*, there are many proposed mechanisms and influencing factors, including lipopolysaccharide (17), hemolysin, and urease in the presence of urea (24). Bacterial invasion may give rise to a relative resistance to antibiotics such as aminopenicillins and persistent infection, due to the save haven provided by the epithelial cells. Here we used an enterocysto-

* Corresponding author. Mailing address: Erasmus University Rotterdam, Josephine Nefkens Institute, Rm. Be 355, Dr. Molewaterplein 50, P.O. Box 1738, 3000 DR Rotterdam, The Netherlands. Phone: 31(0)10-4088488. Fax: 31(0)10-4089386. E-mail: rbmathoera@hotmail.com.

TABLE 1. Antibiotic susceptibilities of five *P. mirabilis* strains[a]

Antibiotic(s)	MIC (μg/ml) for strain[a]:				
	ATCC 49656 (0737000)	AB129 (0336000)	AB474 (0737000)	AB780 (0737000)	AB964 (0733000)
Amikacin	≤2	≤2	4	≤2	4
Amoxicillin-clavulanic acid	≤8	≤8	≤8	≤8	16 (I)
Ampicillin	≥32 (R)	2	4	≥32 (R)	4
Cefotaxime	≤4	≤4	≤4	≤4	≤4
Ceftazidime	≤8	≤8	≤8	≤8	≤8
Cefuroxime-sodium	≤4	≤4	≤4	≤4	≤4
Cefuroxime-axetil	≤4	≤4	≤4	≤4	≤4
Cephalothin	≥32 (R)	4	4	4	4
Ciprofloxacin	≤0.5	≤0.5	≤0.5	≤0.5	≤0.5
Gentamicin	≤0.5	≤0.5	1	≤0.5	1
Imipenem	≤4	≤4	≤4	≤4	≤4
Meropenem	≤2	≤2	≤2	≤2	≤2
Nitrofurantoin	≥128 (R)	≥128 (R)	≥128 (R)	≥128 (R)	≥128 (R)
Norfloxacin	≤4	≤4	≤4	≤4	≤4
Piperacillin-tazobactam	≤8	≤8	≤8	≤8	≤8
Tobramycin	≤0.5	1	≤0.5	≥0.5	1
Trimethoprim-sulfamethoxazole	≤10	≤10	≥320 (R)	≥320 (R)	≥320 (R)

[a] Resistance (R) and intermediate resistance (I) are indicated. The API numbers for each strain are given in parentheses.

plasty in vitro model to study the complex of: infection with urease producing bacteria, intra and extra-cellular crystal formation, adhesion to and invasion of epithelial cells, as well as their influence on antibiotic resistance.

MATERIALS AND METHODS

Bacterial culture. A *P. mirabilis* strain (ATCC 49565) was stored in 15% glycerol at −80°C until needed. Bacteria where cultured in Luria broth–0.05% glycerol until late-log-phase growth before use. Four *P. mirabilis* strains were isolated from patients with an enterocystoplasty (AB129, AB474, AB780, and AB964) by using the API system of identification (Table 1) and Gram staining and then stored in 15% glycerol at −20°C. Genomic DNA was isolated from the five strains by using the Wizard Genomic DNA purification kit (Promega, Madison, Wis.) and a single-primer RAPD-PCR to rule out identical strains. The single 10-nucleotide RAPD-PCR primer (5′-GTGGATGCGA-3′) is routinely used in strain identification. PCR was carried out in 50-μl volumes with 5 to 30 ng of genomic DNA, 0.4 U of SuperTaq DNA polymerase and SuperTaq buffer (Stratech Scientific, Ltd.), and 0.5 mM concentrations of each deoxynucleoside triphosphate with a 0.5 μM concentration of primer. At least four fragments were amplified for each sample in a GeneAmp PCR System 9700 thermocycler programmed for 5 min at 94°C and 40 cycles of 94°C for 30 s, 25°C for 30 s, and 72°C for 45 s. Amplification products were resolved by electrophoresis on a 1.5% agarose gel stained with ethidium bromide (Fig. 1).

Cell culture. We used five intestinal cell lines—Caco-2, HT-29, HT29-18N2, HT29-FU, and HT29-MTX—and one ureter cell line (SV-HUC-1) to study the interactions most common in enterocystoplasties. Caco-2 and HT-29 cell lines were obtained from the American Type Culture Collection (ATCC) and have been passaged for an unknown number of times, but all cells used were within 15 passages. SV-HUC-1 was obtained from the ATCC and has been used from passage 30 to passage 34 to ensure the stability within the cell line. All intestinal cell lines were cultured on Dulbecco minimal Eagle medium (DMEM)-high glucose with glutamine, 10% fetal bovine serum, and 5 mM nonessential amino acids. SV-HUC-1 was cultured on Ham F12 supplemented with 10% fetal bovine serum.

MTT assay. An MTT (thiazolyl blue tetrazolium bromide) assay was performed as described by others to assess the cellular survival in artificial urine in the absence of culture medium by measuring the hexosaminidase activity (15, 16). Cells were cultured in 24-well plates at 50,000 to 100,000 cells per well for 4 days. The cells were overlaid with artificial urine for time periods of between 5 h and 30 min, with or without conditioned medium from a 3-h-old *P. mirabilis* culture in Luria broth at a 1:5 broth/urine ratio. The supernatant was removed, and 200 μl of MTT (Applichem, Darmstadt, Germany) was added at 5 mg/ml. The cells were incubated for 4 h with the MTT solution. The supernatant was then removed, dimethyl sulfoxide was added, and the mixture was shaken for 5 min to extract the formazan formed by the cellular metabolism. The supernatant was transferred to a 96-well flat-bottom plate, and light absorption by formazan was measured in a Bio-Rad platereader with a 570-nm test wavelength and a 690-nm reference wavelength. Similarly, comparisons were made between 3 h of incubation with bacterial secretions in Luria broth compared to Luria broth as an artificial urine supplement for five strains. All MTT assays were performed in triplicate.

Artificial urine composition. Two separate solutions were made and combined at the start of experiments to prevent premature precipitation. Solution A consisted of the following: 1.3 g of sodium citrate, 1.3 g of KH_2PO_4, 2.0 g of sodium oxalate, and 25 g of urea/liter in distilled water. Solution B consisted of the following: 1.3 g of $CaCl_2$, 1.3 g of $MgCl_2$, 9.8 g of NaCl, 4.6 gof $NaSO_4$, 3.2 g of KCl, 2 g of NH_4Cl, and 25 g of urea/liter in distilled water. Both solutions were combined in equal volumes less than 1 h before the experiments. Artificial urine (pH 6.5) without NaCl, $NaSO_4$, and KCl and with 12.5 g of urea/liter with a lower osmolarity of 316 mOsm was also used as a control for osmotic effects on the cell lines.

Cell culture infection. Cells were cultured in 6- or 24-well plates and were infected after they reached confluency. For transmission electron microscopy cells were cultured on 100-μm (pore-size) Melinex (Du Pont Teijin Films Netherlands BV, Rozenburg, The Netherlands) for confocal laser scanning micros-

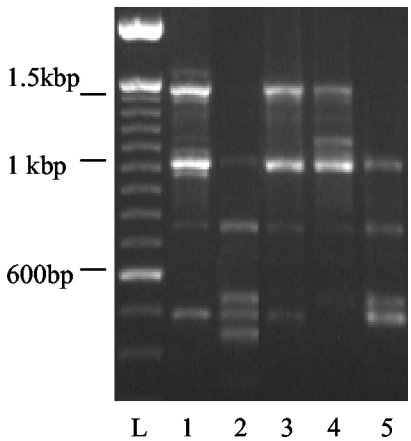

FIG. 1. RAPD-PCR products on 1.5% ethidium bromide agarose gel. Lanes: L, 100-bp standard; 1, AB129; 2, AB474; 3, AB780; 4, AB964; 5, ATCC 49565. All strains have different patterns.

copy on glass coverslips before infection. Artificial urine was added and incubated for 3 h to rise above pH 7.3 and then infected with 150 μl of bacterial suspension (2.5 to 3 McFarlands, ca. 10^5 to 10^6 bacteria) for 3 ml of artificial urine before microscopic evaluation.

Confocal laser scanning microscopy. Infected cells were washed three times with DMEM and maintained at 37°C. A rabbit anti-human colonic mucin (HCM) or rabbit anti-human gastric mucin (HGM) antibody was applied for 15 min and washed three times with DMEM. Anti-HCM and anti-HGM characteristics were previously decribed by Tytgat et. al. (29). Anti-HCM is a rabbit polyclonal antibody raised against purified HCM; it recognizes mainly the mature, fully glycosylated MUC2. Anti-HGM is a rabbit polyclonal antibody raised against purified HGM; it recognizes mainly the mature, fully glycosylated MUC5AC. A monoclonal antibody against *P. mirabilis* (Biogenesis; Nuclilab) was added, incubated for 15 min and washed three times with DMEM. A fluorescein isothiocyanate (FITC)-labeled anti-rabbit antibody (Caltac Laboratories, Burlingame, Calif.) was applied, incubated for 15 min, washed thoroughly with DMEM, and monitored by a TRITC (tetramethyl rhodamine isothiocyanate)-labeled anti-mouse antibody (Dako A/S, Copenhagen, Denmark). Images were made with a Zeiss LSM 410 laser scanning confocal microscope (Zeiss, Oberkochen, Germany). A 488-nm Ar laser was used to excite TRITC-labeled antibodies and a 633 Kr laser without a filter to visualize the reflection of the crystals. The TRITC signal was passed through a 510- to 540-nm bandpass filter. An overlay of the FITC signal was done by using the 488-nm laser and a 560-nm beam splitter to separate the FITC from the TRITC signal, showing bacterial infection and crystal formation. Viable stain Syto16 was used instead of anti-mucin antibodies, omitting the last washing step, to show viable epithelial cells and determine bacterial invasion. Experiments were performed in triplicate except bacterial invasion assessment, which was performed twice to confirm previous findings. A second observer evaluated a representative selection of images.

Transmission electron microscopy. Cells were cultured on a Melinex sheet to attain transferable monolayers until they reached confluency, and they were then fixed in 1% glutardialdehyde–4% formaldehyde in 0.1 M phosphate-buffered saline (PBS; pH 7.2) at 4°C for at least 2 h before processing. Detached cells were collected and centrifuged to a pellet before processing. Samples were washed in 0.1 M PBS (pH 7.2) at 4°C for 12 h, followed by a secondary fixation in 1% osmium tetraoxide–1.5% $K_4Fe(CN)_6$ in 0.1 M PBS (pH 7.2). Samples were washed twice in distilled water for 30 min and dehydrated in ethanol 50, 50, 70, 70, 90, 90, 96, and 96% for 10 min and twice in ethanol 100% for 15 min. Samples were impregnated in equal volumes of epoxy resin (LX112) and ethanol 100% for 60 min at room temperature, followed by pure Epoxy resin (LX112) for 60 min at 37°C. Resin was allowed to polymerize for 12 h at 60°C, after which the Melinex sheet was removed.

Sectioning of blocks was performed on a type LKB IV ultramicrotome at 40 nm, and then the sections collected on a copper 200-mesh grid. Sections were incubated with 6% uranyl acetate for 10 min, followed by lead citrate for 1 min, before they were viewed under a Philips Morgangi 268 transmission electron microscope connected to a charge-coupled device camera (MegaView II).

Gentamicin invasion assay. Cells were cultured in 24-well plates until reaching confluency and then incubated with *P. mirabilis* in Hanks balanced salt solution (HBSS) for 3 h. Cells were washed twice with HBSS to remove free bacteria and incubated with 0.01% gentamicin in PBS for 1 h to kill accessible bacteria. The monolayers were washed eight times with PBS to remove all gentamicin and lysed in poly-L-lysine (Sigma-Aldrich P1524) for 5 min. A 1/10 dilution series was made, plated on blood-agar plates, and incubated at 37°C for 24 h. Experiments were performed in triplicate to reveal bacterial survival in epithelial cells.

RASA. The relative antibiotic susceptibility assay (RASA) procedure followed the gentamicin invasion assay except for three major changes. First, the incubation time with the antibiotic was increased from 1 to 18 h. Second, a panel of commonly used antibiotics was applied at concentrations, reflecting the calculated expected urinary excretions in pediatric urology for a 10-year-old child weighing 30 kg. The following antibiotics and amounts were used: amoxicillin, 450 μg/ml; amoxicillin (600 μg/ml)-clavulanic acid (60 μg/ml) (augmentin); gentamicin, 90 μg/ml; trimethoprim (46 μg/ml)-sulfamethoxazole (230 μg/ml) (cotrimoxazole); ciprofloxacin, 300 μg/ml; nitrofurantoin, 50 μg/ml; and metronidazole, 20 μg/ml. Third, lysates were plated on MacConkey agar instead of blood agar to enable colony counting and then incubated at 37°C for 24 h. For a panel of five bacterial strains, the resistance against a specific antibiotic ($n = 8$ [including DMEM control]) was tested both in the presence and in the absence of a specific cell line ($n = 6$). Overall, the numbers of CFU were counted for $5 \times 2 \times 6 \times 8 = 480$ different situations. For each combination of bacterial strain and antibiotic, we calculated the ratio of CFU in the presence (CFU_{cell+}) and absence (CFU_{cell-}) of cells, i.e., CFU_{cell+}/CFU_{cell-}. This ratio was considered to be increased at a cutoff point of 10. For the statistical analysis of the differences between the cells present and the cells absent, we used the average of the ratios obtained for the five bacterial strains in a paired-samples *t* test. These stringent conditions helped us to answer questions as to whether bacteria can resist antibiotic treatment by invading cells and which antibiotics would still be suitable.

Flow cytometric analysis of infected epithelial cells. All flow cytometric measurements of HCM, HGM, caspase-3, and bacteria were performed separately by using material from the same infected sample. Infected cells were incubated in 70% ethanol for 30′ and scraped, followed by overnight incubation at room temperature in 2% paraformaldehyde–2% formaldehyde to fix the cells and bacteria. Fixed cells were washed twice with PBS; the first antibody in 0.5% bovine serum albumin–PBS was applied against *P. mirabilis*, HCM, HGM, or caspase-3 and incubated for 1 h at 37°C. Cells were washed with PBS twice, and a secondary FITC-labeled antibody was applied and incubated for 1 h at 37°C, after which the cells were washed twice with PBS before measurement. After the first measurement trypan blue was added to quench an intracellular FITC signal and incubated for 30 min, the cells were then washed twice with PBS and measured again. The decrease in signal determines the contribution of membrane-bound and intracellular signal. Antibody dilutions (1:200) were used. Pearson correlation was used to analyze protein expression by the mean FL-1 count in relation to the RASA.

RESULTS

Bacterial identification. Bacterial strains with similar API codes (Table 1) were identified as unique strains by RAPD-PCR (Fig. 1).

Confocal laser scanning microscopy. In confocal laser scanning microscopy, epithelial cells of ca. 7 μm, expanded in size after infection with *P. mirabilis* and a colocalization of mucins expressed on the cellular membrane and bacterial adhesion, was demonstrated for HCM and for HGM (Fig. 2C and D). Furthermore, intracellular crystal formation was demonstrated for all cell lines, and intracellular invasion was confirmed (Fig. 2A and B). In the intestinal cell lines cytoplasmic colonies are observed (Fig. 2B) opposed to single cell invasion in the ureter cell line (Fig. 2A). Both HCM and HGM appeared as granules in cells and membrane-associated mucins on the cells, indicating the mature mucine form (Fig. 2C and D). Colocalization of HCM and HGM with *P. mirabilis* occurred in all cell lines and is visible in Fig. 2C and D as a yellow-orange signal. For a better assessment of this colocalization, the single colocalization signal is shown in black for the same areas in Fig. 2E and F. Large cells were observed for HT29-18N2 with a large number of cytoplasmic bacteria.

Transmission electron microscopy. Cellular adhesion (Fig. 3B), cytoplasmatic colonies and invasion by *P. mirabilis* surrounded by a double membrane was observed in intestinal cell lines (Fig. 3C) with intracytoplasmatic crystal formation and crystal adhesion to the cellular membrane. The urothelial cell line showed fewer bacteria and always bacteria that had invaded into the cells without a double membrane (Fig. 3D) and large crystal deposits on and in the cell (Fig. 3A). Occasionally, intramitochondrial (Fig. 3E) crystal formation was observed. The results are presented in Table 2. The results indicate that bacterial infection in artificial urine of 316 mOsm enhances the formation of crystals (intracellular and in mitochondria) in conjunction with enhanced bacterial invasion. For HT29-18N2, large-scale destruction of cells was noted with large cells and bacterial colonies contained by a double membrane. Infected epithelial cells showed loss of nuclear staining and density, indicating damage.

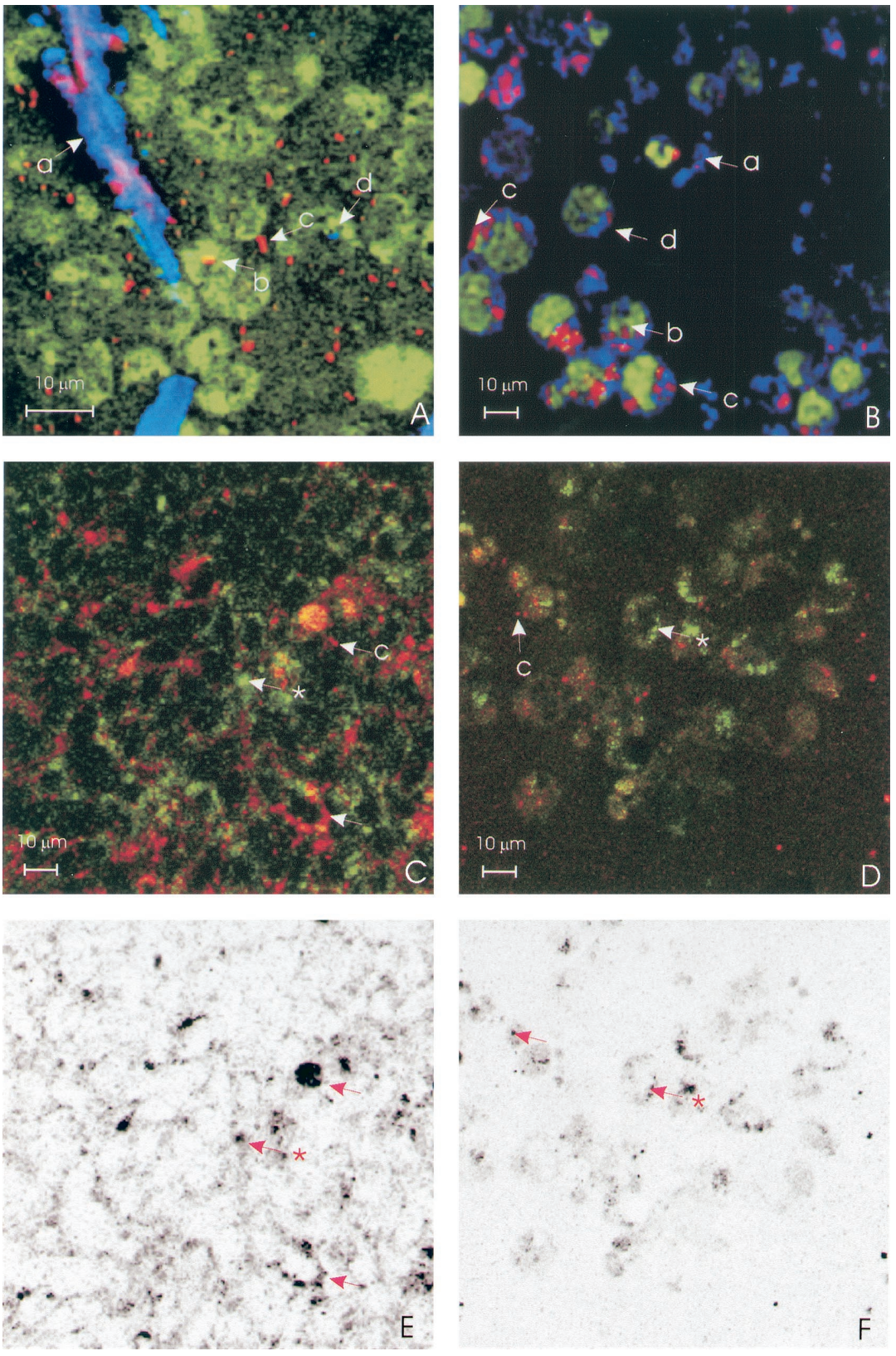

FIG. 2. Confocal laser scanning microscopy images (all images at ×800 magnification). Bacteria are always red. (A) SV-HUC-1 cell line stained with viable stain Syto-16 with reflecting crystals (blue or purple). (B) HT29-MTX stained with viable stain Syto-16 (green), with reflecting crystals (blue). The letters a, b, c, and d refer to extracellular crystals, intracellular bacteria, extracellular bacteria, and intracellular crystals, respectively. (C) HT29-MTX cell line showing HCM in green and colocalization in yellow (⁕, HCM along the cellular membrane; arrow, bacterial and HCM colocalization). (D) HT29-MTX cell line showing HGM in green and colocalization in yellow (⁕, HGM without bacterial colocalization; arrow, HGM with bacterial colocalization). The yellow colocalization signal is produced by a simultaneous red TRITC and green FITC signal. (E) Colocalization signal of *P. mirabilis* and HCM of panel C indicated in black. (F) Colocalization signal of *P. mirabilis* and HGM of panel D indicated in black.

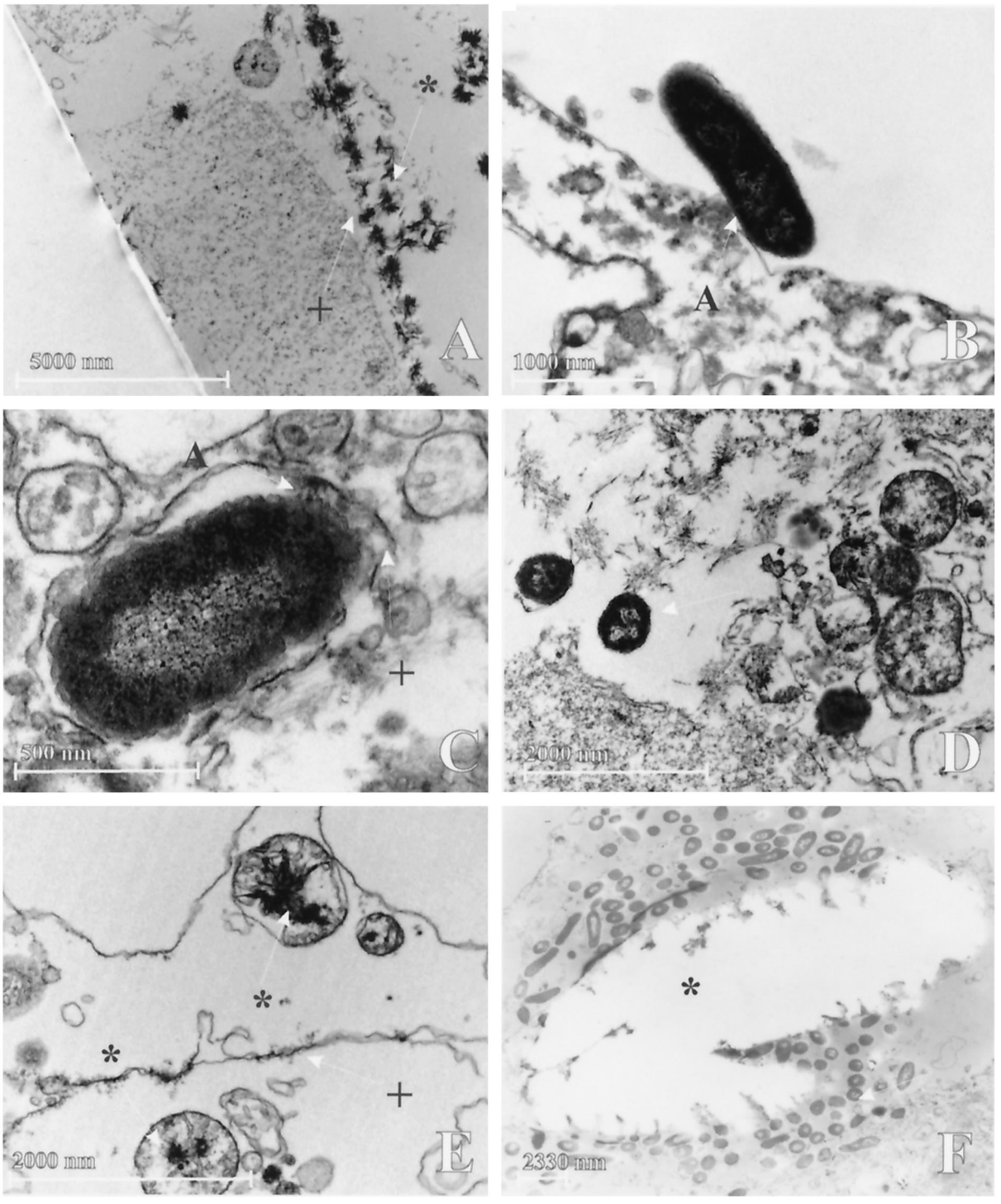

FIG. 3. Transmission electron microscopy. (A) Crystals on SV-HUC-1 cell surface (magnification, ×2,800); (B) bacterial adhesion to the cellular surface of HT29-MTX under conditions without artificial urine (magnification, ×22,000); (C) invasion in HT29-FU with double membrane (magnification, ×44000); (D) bacterial invasion in SV-HUC-1, without a double membrane (magnification, ×14,000); (E) crystal formation inside cellular organelle of HT29-FU, probably destroyed mitochondrium (magnification, ×18,000); (F) Crystal ghost in HT29-MTX, with large cytoplasmatic colony of *P. mirabilis* surrounding the crystal (magnification, ×3,000). Arrows without any symbols indicate bacteria. Arrows with a symbol (panel A) indicate bacterial adhesion to the double membrane. The double membrane is indicated by "+," and crystals are indicated by an asterisk.

TABLE 2. Transmission electron microscopy results with various culture and infection conditions[a]

Evaluation parameter and cell line	Culture and infection conditions			
	DMEM	Artificial urine	DMEM + *P. mirabilis*	Artificial urine + *P. mirabilis*
Crystal adhesion				
Caco-2	−	+	−	+
SV-HUC-1	−	−	−	+
HT29	−	+	−	−
HT29-1 8N2	−	−	−	−
HT29-FU	−	−	−	−
HT29-MTX	−	−	−	+
Intracytoplasmic crystal formation				
Caco-2	−	+	−	+
SV-HUC-1	−	−	−	+
HT29	−	+	−	+
HT29-1 8N2	−	−	−	+
HT29-FU	−	+	−	+
HT29-MTX	−	−	−	+
Intramitochondrial crystal formation				
Caco-2	−	−	−	+
SV-HUC-1	−	−	−	+
HT29	−	−	−	−
HT29-1 8N2	−	−	−	−
HT29-FU	−	−	−	+
HT29-MTX	−	−	−	+
Bacterial adhesion				
Caco-2	−	−	+	+
SV-HUC-1	−	−	+	+
HT29	−	−	+	−
HT29-1 8N2	−	−	−	+
HT29-FU	−	−	−	+
HT29-MTX	−	−	+	−
Bacterial invasion				
Caco-2	−	−	−	+
SV-HUC-1	−	−	+	+
HT29	−	−	−	+
HT29-1 8N2	−	−	−	+
HT29-FU	−	−	−	+
HT29-MTX	−	−	−	+

[a] Cell pellets and monolayer cultures were used in infected artificial urine conditions; all other conditions were evaluated in monolayer conditions (+, present; −, absent).

RASA and gentamicin invasion assay. After a vigorous washing to remove all antibiotic and free bacteria, viable bacteria were found upon cell lysis for all cell lines tested, thus confirming bacterial invasion. The RASA showed that this cellular invasion provides the bacteria with a relative protection against the antibiotics cotrimoxazole and amoxicillin-clavulanic acid. DMEM acts as a control for bacterial growth without any inhibition in the presence of cells. Amoxicillin acts as a control for the amoxicillin content in augmentin to assess clavulanic acid. Amoxicillin does not show diminished effectivity in the presence of cells, and neither metronidazole nor nitrofurantoin exhibits a significant change in effectivity according to a paired-sample *t* test, although augmentin (amoxicillin-clavulanic acid) does. Ciprofloxacin and gentamicin still seem to be suitable antibiotics in the presence of epithelial cells.

The results of the RASA are presented in Table 3.

MTT assay. Cell survival decreased over time in the presence of artificial urine instead of normal culture medium. The hexosaminidase activity dropped to ca. 50% in all cell lines with or without the added preconditioned Luria broth in 3 h. The cells showed a hexosaminidase activity after 3 h, a finding comparable to conditions with (Fig. 4) or without (Fig. 5) the preconditioned Luria broth; some cell lines with conditioned medium from certain bacterial strains, however, showed differences compared to a blank sample without conditioned medium. These readings were always higher in the Caco-2, HT29, and HT29-FU cell lines and were always significantly higher in the HT29-FU cell line, whereas they were only significant for the SV-HUC-1 cell line in combination with the ATCC 49565 strain. Significant differences are marked in Fig. 5.

Flow cytometric analysis of infected epithelial cells. On average over all epithelial cell lines, 23% of the bacteria were intracellularly located. A total of 23.2% were found in Caco-2 cells, 26.7% were found in SV-HUC-1 cells, 22.7% were found in HT29 cells, 0.5% were found in HT29-18N2 cells, 31.8% were found in HT29-FU cells, and 24.1% were found in HT29-MTX cells. The HT29-18N2 values for bacterial invasion were very low due to large-scale destruction of the epithelial cells and high permeability for trypan blue, which shows aberrant results for the AB780 strain only. The results are presented in Fig. 6. Of all HCM and HGM expressed by the cells, most was present on the cellular surface; only a small fraction was contained as granules in the cell. A total of 60 to 95% of the HCM and HGM was expressed on the cell surface but did not show significant differences among the cell lines. Of the more than 5,000 correlations analyzed between flow cytometric data, RASA, and the MTT assay, the relevant significant results are presented as a meta-analysis in Table 4. Caspase-3 expression was not correlated with hexosaminidase activity, bacterial invasion, or MUC2 or MUC5AC expression. Hexosaminidase activity was not correlated with bacterial invasion.

DISCUSSION

Conditions as they exist in the augmented bladder, especially in the presence of intestinal cells and their secretions in the presence of urine, enhances bacterial infection and invasion. Often *P. mirabilis* infection of the augmented bladder is difficult to treat and leads to stone formation. *P. mirabilis* can invade epithelial cells and survive intracellularly (3, 5, 25, 32, 33, 34). It is not known if this affects antibiotic effectivity. We studied the effect of bacterial invasion by *P. mirabilis* on antibiotic susceptibility and intracellular crystal formation in conditions modeled to the environment present in enterocystoplasties. The RASA was developed in artificial urine for this purpose. Artificial urine is a useful defined culture medium for the growth of *P. mirabilis* (4). The meta-analysis of a number of control parameters for bacterial survival in cells, including the MICs, are useful in evaluation of the data gathered from our RASA. The data allow us to propose the scheme for bacterial invasion or survival shown in Fig. 7. Interventional studies must be performed to test the validity of the scheme

In the present study artificial urine enhances invasion of

TABLE 3. RASA results[a]

Cell line	Strain	RASA results															
		DMEM		Amoxicillin		Augmentin		Cotrimoxazole		Ciprofloxacin		Gentamicin		Nitrofurantoin		Metronidazole	
		Group	Mean (SE); P^b	Group	Mean (SE); P^b	Group	Mean (SE); P^b	Group	Mean (SE); P^b	Group	Mean (SE); P^b	Group	Mean (SE); P^b	Group	Mean (SE); P^b	Group	Mean (SE); P^b
Caco-2	AB129	+	0.60 (0.51); 0.305	−	0.80 (0.66); 0.294	−	0.80 (0.58); 0.242	+	**1.0 (0.32); 0.034***	−	−0.40 (0.68); 0.587	−	0.60 (0.40); 0.208	−	1.0 (0.63); 0.189	+	**1.0 (0.32); 0.034***
	AB474	+		+		+		+		+		+		+		+	
	AB780	−		−		+		+		−		−		+		+	
	AB964	+		+		+		+		+		+		+		+	
	ATCC 49565	−		+		−		−		−		−		+		−	
SV-HUC-1	AB129	−	0.62 (0.39); 0.189	−	0.02 (0.44); 0.966	+	**1.42 (0.24); 0.004***	−	0.02 (0.01); 0.178	+	−0.18 (0.36); P=0.646	−	0.02 (0.01); 0.178	−	0.02 (0.01); 0.178	+	0.02 (0.01); 0.178
	AB474	+		+		+		−		+		+		+		−	
	AB780	+		+		+		−		+		+		+		+	
	AB964	−		+		+		+		−		−		−		−	
	ATCC 49565	−		−		+		−		−		−		−		−	
HT29	AB129	+	0.40 (0.24); 0.178	−	0.60 (0.24); 0.070	−	M=0.60 Se=(0.40); P=0.208	−	0.60 (0.24); 0.070	−	−0.20 (0.73); 0.799	−	0.20 (0.66); 0.778	−	0.20 (0.86); 0.828	+	0.80 (0.37); 0.099
	AB474	+		−		+		+		+		+		+		+	
	AB780	−		+		+		+		+		−				+	
	AB964	−		+		−		+		−		+		−		−	
	ATCC 49565	−		+		−		−		−		−		+		−	
HT29-18N2	AB129	−	1.0 (0.44); 0.086	−	1.0 (0.44); 0.086	−	**4.20 (0.58); 0.002***	−	0.60 (0.39); 0.202	−	0.00 (0.02); 1.0	−	0.20 (0.19); 0.347	−	0.60 (0.39); 0.202	−	0.60 (0.67); 0.424
	AB474	+		+		−		−		−		−		−		−	
	AB780	+		+		+		−		−		−		−		−	
	AB964	−		+		+		−		−		−		−		+	
	ATCC 49565	−		−		+		−		−		−		−		−	
HT29-FU	AB129	+	0.80 (0.37); 0.099	−	0.40 (0.24); 0.178	+	1.0 (0.55); 0.142	+	**1.20 (0.20); 0.004***	−	−0.20 (0.49); 0.704	−	0.20 (1.02); 0.854	−	0.20 (0.86); 0.828	+	1.0 (0.55); 0.142
	AB474	+		+		+		+		+		+		+		+	
	AB780	−		+		+		+		−		−		−		+	
	AB964	−		−		−		+		−		−		−		+	
	ATCC 49565	+		−		−		+				−		+		−	
HT29-MTX	AB129	+	0.20 (0.37); 0.621	−	0.00 (0.55); 1.0	−	0.20 (0.58); 0.749	+	**0.80 (0.20); 0.016***		−0.40 (0.68); 0.587	−	0.20 (0.86); 0.828	−	−0.40 (0.75); 0.621	+	0.60 (0.51); 0.305
	AB474	−		+		+		+		−		+		+		−	
	AB780	−		+		+		+		+		+		−		+	
	AB964	+		−		−		+		−		−		−		+	
	ATCC 49565	−		−		−		−		−		−		−		−	

[a] The logarithmic numbers of CFU of lysed cells/logarithmic numbers of CFU in cell-free controls were divided into two groups of ≤1 (indicated by "−") and >1 (indicated by "+") and used in a binomial test to evaluate the possible effectivity of antibiotics. The numbers of CFU were read from MacConkey agar plates. The logarithmic colony counts were used in paired *t* tests with the corresponding cell-free control to assess *P. mirabilis* resistance to antibiotic therapy in the presence of cells. Mean, the mean of paired differences. *P*, *P* value in paired *t* test. *, Significant in paired *t* test (indicated by boldface). Boldfacing also indicates possible effective antibiotics in this cell line (binomial test, all controls are negative; samples are positive when the colony count exceeds that of the corresponding control).

[b] The overall mean, standard error, and *P* value for each subgroup of data is provided.

bacteria and intracellular crystal formation. The presence of crystals in cellular organelles, i.e., intramitochondrial crystals confirms their intracellular origin. The large Ca^{2+} stores in mitochondria and the endoplasmic reticulum (21, 31) may explain the cellular location of crystals when the pH level rises above 7.3 and the solubility of calcium phosphate is exceeded. Mitochondrial damage may then lead to increased cytosolic calcium levels and precipitation at other cell sites. Bacterial activity and mechanical damage by crystals eventually leads to nuclear destruction and a disruption of calcium levels (12, 21), with a more diffuse distribution of crystals throughout the epithelial cytoplasm, as was observed in electron microscopy. The rise in the pH level was caused by urease-producing *P. mirabilis* strains. These strains invaded the cells and formed a microenvironment, which supported the formation of crystals.

We hypothesized that microcolony formation inside epithe-

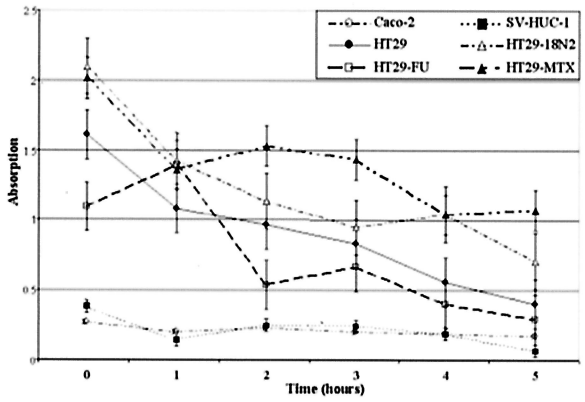

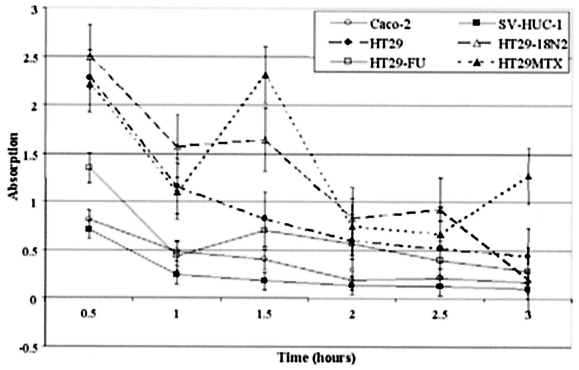

FIG. 4. (A) MTT assay of epithelial cells incubated with artificial urine monitored over time. (B) MTT assay of epithelial cells incubated with artificial urine and conditioned Luria broth by *P. mirabilis* ATCC 49565 monitored over time. Error bars represent the standard error of the mean.

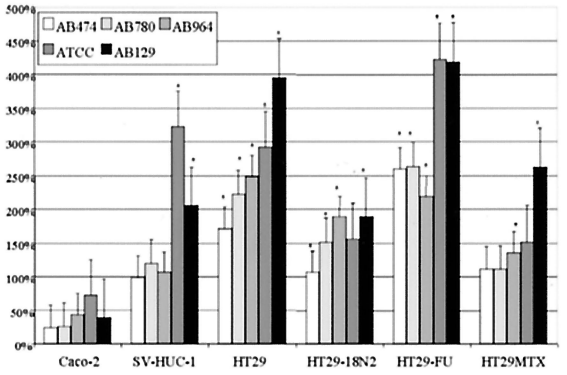

FIG. 5. MTT assay of epithelial cells incubated for 3 h with artificial urine supplemented with conditioned Luria broth by five *P. mirabilis* strains for 3 h compared to artificial urine and unconditioned Luria broth. Incubation with unconditioned Luria broth and artificial urine for 3 h was set as 100%. Values of >100% outside the standard error bars are indicated as significant (*). Histograms represent average values of three MTT assays. Error bars represent the standard error of the mean.

lial cells protects against antibiotic treatment, in particular against antibiotics that have a concentration-dependent activity, a low membrane permeability, or for which *P. mirabilis* has already acquired a relative resistance. In vivo epithelial invasion would create a bacterial pool from which the next cycle of infection can originate. An additional double membrane surrounded bacteria in the intestinal cell lines, providing an extra barrier for antibiotics to pass in addition to the cellular cytoplasm, suggesting that *P. mirabilis* was better protected inside intestinal cells. The RASA test (wherein the extracellular bacteria were removed) shows that intracellular bacteria better survive treatment with the antibiotics cotrimoxazole and amoxicillin-clavulanic acid, against which one or more strains were already (relatively) resistant. Invasion was confirmed in

TABLE 4. Meta-analysis of infection and survival data[a]

First factor		Direction of correlation	Second factor		*P*
Type	Cell line		Type	Antibiotic	
MUC5AC	HT29-MTX	Negative	Bacterial invasion		0.048
HCM	HT29-MTX	Negative	Bacterial invasion		0.023
MUC5AC	HT29-MTX	Negative	Bacterial survival	Ciprofloxacin	0.025
MUC5AC	HT29-MTX	Negative	Bacterial survival	Gentamicin	0.042
Hexosaminidase	HT29-MTX	Positive	Bacterial survival	Metronidazole	0.029
MUC5AC	HT29	Positive	HCM		0.049
Caspase-3	HT29	Positive	Bacterial survival	DMEM	0.007
Caspase-3	HT29	Negative	Bacterial survival	Amoxicillin	0.007
MUC5AC	SV-HUC-1	Positive	Bacterial invasion		0.042
Caspase-3	SV-HUC-1	Positive	Bacterial survival	Nitrofurantoin	0.008
Bacterial invasion	SV-HUC-1	Positive	Bacterial survival	Metronidazole	0.032
HCM	Caco-2	Negative	Hexosaminidase		0.038
HCM	Caco-2	Positive	Bacterial survival	Amoxicillin	0.006
Bacterial invasion	HT29-18N2	Negative	Bacterial survival	DMEM	0.026
Bacterial invasion	HT29-18N2	Negative	Bacterial survival	Amoxicillin	0.027
Bacterial invasion	HT29-18N2	Negative	Bacterial survival	Augmentin	0.027
Bacterial invasion	HT29-18N2	Negative	Bacterial survival	Ciprofloxacin	0.025
Bacterial invasion	HT29-18N2	Negative	Bacterial survival	Metronidazole	0.027

[a] Bacterial invasion, caspase-3 expression, and MUC5AC and HCM levels were determined by flow cytometric analysis. Bacterial survival was determined by RASA, and the hexosaminidase activity was determined by the MTT assay. The meta-analysis of data was performed by using the Pearson correlation. Correlations were significant ($P < 0.05$) in a two-tailed test.

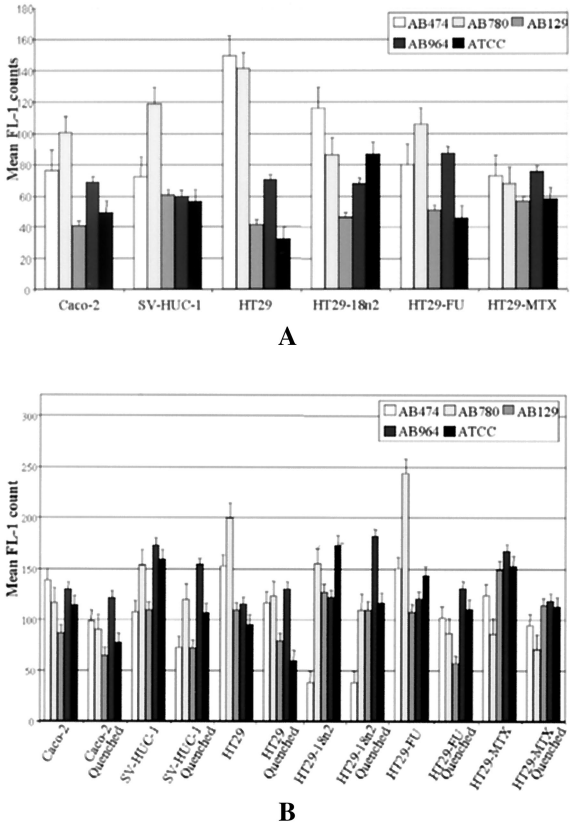

FIG. 6. (Top panel) Flow cytometric analysis of caspase-3 expression in epithelial cells infected with five *P. mirabilis* strains. (Bottom panel) Bacterial adhesion (quenched) and total bacterial infection of epithelial cells. Bacterial invasion was regarded to be the difference between the quenched (extracellular) data and the total *P. mirabilis* infection. The error bars represent the standard error of the mean.

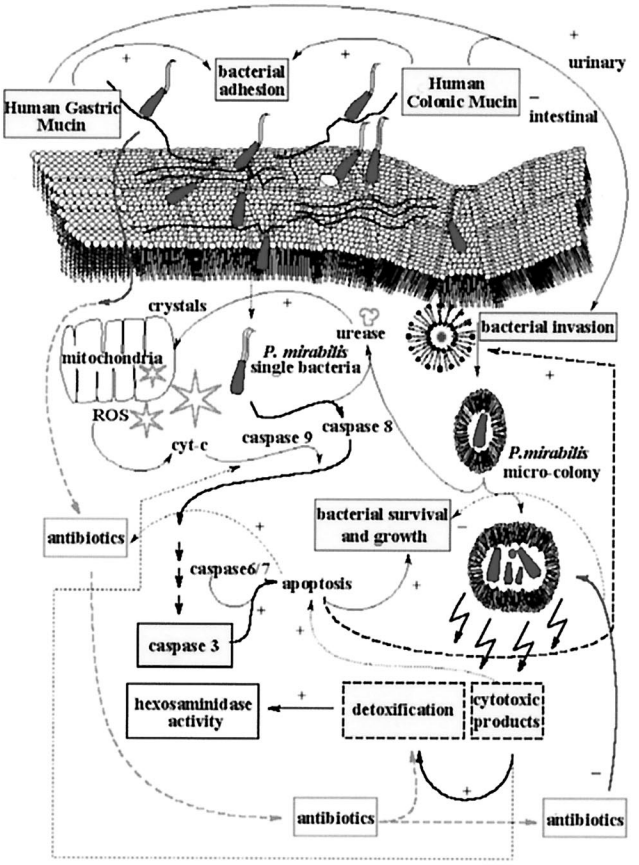

FIG. 7. Schematic presentation of our interpretation of the data and meta-analysis. The diagram shows bacterial adhesion and invasion of epithelial cells, with possible mechanisms of factors influencing the outcome of the RASA. Both bacteria and crystals can start apoptosis by inducing cellular stress. Bacterial invasion is either inhibited or enhanced by adhesion to HGM or HCM. Bacterial invasion and apoptosis may enhance antibiotic effectivity by increasing the permeability of the cellular membrane after increasing the permeability of the nuclear membrane. Mitochondrial damage will enhance the bacterium-induced apoptosis of the epithelial cell. *P. mirabilis* will invade the cell and form microcolonies, which are protected from antibiotics in the cytoplasm by the microenvironement formed within the double membrane formed in intestinal cell lines. In SV-HUC-1, single bacteria are found without the protection of a double membrane (left), whereas in the intestinal cell lines a double membrane was found surrounding invaded *P. mirabilis* bacteria and microcolonies (right).

flow cytometric data. On average, 23% of the bacteria were located inside intact cells for all cell lines tested except for HT29-18N2, which showed massive cell destruction. This factor may be beneficial for the epithelial cells since increased cell membrane permeability makes *P. mirabilis* lose their safe haven, as in HT29-18N2.

Self-destruction could be a way for the cells to deprive the bacteria of their protection. In infected cells mitochondrial swelling and destruction was visible. This suggests an apoptosis mechanism involving the radical oxygen species → cytochrome *c* → caspase-9 → caspase-3 pathway (28).

Expression of caspases due to infection would decrease bacterial survival for amoxicillin in HT29 cells but, according to our data, does not significantly increase bacterial invasion. Only in control antibiotics and DMEM did caspase-3 correlate with increased bacterial survival. This suggests that cellular membrane permeability is increased. Overall, neither a significant effect of apoptosis on RASA or a direct correlation between caspase-3 and bacterial invasion was found. It may be that *P. mirabilis* counteracts the effect of apoptosis since it produces an iron-dependent superoxide dismutase that handles radical oxygen species. Also, caspase-3 can promote nuclear membrane permeability without increasing cellular permeability (12), as is observed by electron microscopy.

The presence of artificial urine and the absence of normal culture medium affected the cellular metabolism and increased the invasion of epithelial cells. However, bacterial secretions that constitute a stress situation for the cell only marginally affected the metabolism of epithelial cells. When invasion is very efficient, such as for the HT29-18N2 cell line, there is rapid cell destruction. Thus, we investigated the cellular reaction to invasion by using hexosaminidase activity as a marker for cellular survival and metabolic activity (6, 8). Hexosaminidase, a detoxification enzyme (15) in the lysosomal degradative pathway, may be activated by proinflammatory stimuli (27). When hexosaminidase function was enhanced, lysosomal degradation and bacterial survival with cell-protective metronidazole increased (18).

Epithelial mucins have a dual effect in the invasion of *P. mirabilis*, depending on the cell line. In HT29-MTX cells, bacterial invasion is decreased by MUC2 and MUC5AC, and colony formation occurs, which could indicate phagocytosis of the cellular membrane with the bacteria in which the mucins act as a bacterial barrier. In the ureter cell line SV-HUC-1 bacterial invasion occurs as single bacterium and is positively correlated with MUC5AC expression, indicating a receptor function. Mucins such as MUC2 could also function as a barrier to antibiotics such as amoxicillin in Caco-2 cells. Bacterial secretions seem to induce metabolic activity in the cells, which may help the destruction of *P. mirabilis* and the detoxification of antibiotics. It seems that excretions from *P. mirabilis* induce a cellular response in certain HT29 cell lines that requires a higher metabolic activity of the epithelial cell. The HT29 and HT29-FU subclones and Caco-2 cells that are activated in the presence of bacterial secretions are known to produce relatively more MUC2 and MUC5AC (22). Mucin production may be involved as a defense mechanism against interaction with *P. mirabilis* lipopolysaccharide, as has been reported for other bacteria (20, 21) and may be regulated similarly (19). Recycling of the cellular membrane, which is unrelated to the bacterial agent, incorporates substances from the cellular membrane such as mucins, as described for MUC1 (1). On the other hand, mucins may inhibit phagocytosis by polymorphonuclear leukocytes in the lung (30). It is not clear from the present study how different mucin types interact at a molecular level with bacteria, but there seems to be a difference in the invasion capability of *P. mirabilis* according to the type of epithelium, i.e., urothelium or intestinal epithelium, related to mucin expression.

Conclusion. The overall interpretation of our data is depicted in Fig. 7. Bacterial invasion in epithelial cells is enhanced by the enterocystoplasty environment with urine, mucin, and intestinal cells. The invasion into urothelial and intestinal cells shows different aspects, resulting in single-membrane and double-membrane protection, respectively. This protection induces a relative resistance of *P. mirabilis* to the antibiotics cotrimoxazole and amoxicillin-clavulanic acid. Gentamicin and ciprofloxacin are the the most effective antibiotics in the presence of epithelial cells, and nitrofurantoin also seems to be more effective in the presence of these cells. *P. mirabilis* thrives better inside the cell when there are antibiotics in the culture medium and better outside the cell when there is no selection pressure from antibiotics. Resistance to cotrimoxazole and, of course, nitrofurantoin is also often found clinically (7). Resistance to amoxicillin-clavulanic acid and ciprofloxacin is less frequent. *P. mirabilis* appears to interact with mucins such as MUC2 and MUC5AC in the adhesion to epithelial cells preceding invasion but is not necessarily internalized with these mucins. These mucins act differently according to the origin of the cell type and may relate to the different microbiological function of intestinal and urinary epithelium. HCM is equivalent to the mature form of MUC2, and HGM is equivalent to the mature form of MUC5AC (29). *P. mirabilis* appears to reproduce more effectively in intestinal cells than in ureter cells by the formation of cytoplasmic colonies. This may help explain the persistence of *P. mirabilis* in enterocystoplasties under antibiotic therapy. The infection stones in the augmented bladder may start as intracellular crystals (ca. 7 μm according to confocal laser scanning microscopy) at the surface of the bacterial capsule. These crystals are protected from washout by voiding and also enhance bacterial survival when they reach a larger size, according to the generally accepted safe-haven theories for biofilms and urinary calculi.

Further research, e.g., on interactions of bacterial molecules with MUC2 and MUC5AC, must show whether fighting cell invasion can provide a more effective treatment of *P. mirabilis* infection.

ACKNOWLEDGMENTS

We acknowledge the expert assistance of P. Van den Heul and especially A. W. De Jong for help with the transmission electron microscopy sectioning and imaging and A. Houtsmüller for his assistance with confocal laser scanning microscopy imaging. ing. C. van der Schee provided assistence with the RAPD-PCR. W. C. J. Hop (Department of Epidemiology and Biostatistics) provided assistance with statistical analysis of data. Anti-HCM and anti-HGM were gifts from A. W. C. Einerhand, Department of Pediatrics, Erasmus University (Rotterdam). The HT29-FU and HT29-MTX were gifts from T. Lesuffleur (INSERM U505, Centre de Recherche Biomédicales des Cordeliers, Paris, France), and HT29-18N2 was a gift from Daniel Louvard (UMR144; CNRS-Institut Curie, Paris, France).

REFERENCES

1. **Altschuler, Y., C. L. Kinlough, P. A. Poland, J. B. Bruns, G. Apodaca, O. A. Weisz, and R. P. Hughey.** 2000. Clathrin-mediated endocytosis of MUC1 is modulated by its glycosylation state. Mol. Biol. Cell **11:**819–831.
2. **Barroso, U., Jr., R. Jednak, P. Fleming, J. S. Barthold, and R. Gonzalez.** 2000. Bladder calculi in children who perform clean intermittent catheterization. BJU Int. **85:**879–884.
3. **Braude, A. I., and J. Siemienski.** 1960. Role of bacterial urease in experimental pyelonephritis. J. Bacteriol. **80:**171–179.
4. **Brooks, T., and C. W. Keevil.** 1997. A simple artificial urine for the growth of urinary pathogens. Lett. Appl. Microbiol. **24:**203–206.
5. **Chippendale, G. R., J. W. Warren, A. L. Trifillis, and H. L. T. Mobley.** 1994. Internalization of *Proteus mirabilis* by human renal epithelial cells. Infect. Immun. **62:**3115–3121.
6. **Cole, S. P. C.** 1986. Rapid chemosensitivity testing of human lung tumor cells using the MTT assay. Cancer Chemother. Pharmacol. **17:**259–263.
7. **Daza, R., J. Gutierrez, and G. Piedrola.** 2001. Antibiotic susceptibility of bacterial strains isolated from patients with community-acquired urinary tract infections. Int. J. Antimicrob. Agents **18:**211–215.
8. **Denizot, F., and R. Lang.** 1986. Rapid colorimetric assay for cell growth and survival. J. Immunol. Methods **89:**271–277.
9. **Duel, B. P., and R. Gonzalez, and J. S. Barthold.** 1998. Alternative techniques for augmentation cystoplasty. J. Urol. **159:**998–1005.
10. **Dumanski, A. J., H. Hedelin, A. Edin-Liljegren, D. Beauchemin, and R. J. C. McLean.** 1994. Unique ability of the *Proteus mirabilis* capsule to enhance mineral growth in infectious urinary calculi. Infect. Immun. **62:**2998–3003.
11. **Ebisuno, S., T. Komura, K. Yamagiwa, and T. Ohkawa.** 1997. Urease induced crystallizations of calcium phosphate and magnesium ammonium phosphate in synthetic urine and human urine. Urol. Res. **25:**263–267.
12. **Faleiro, L., and Y. Lazebnik.** 2000. Caspases disrupt the nuclear-cytoplasmic barrier. J. Cell Biol. **151:** 951–959
13. **Griffith, D. P.** 1978. Struvite stones. Kidney Int. **13:**372–382.
14. **Kaefer, M., M. S. Tobin, W. H. Hendren, S. B. Bauer, C. A. Peters, A. Atala, A. H. Colodny, J. Mandell, and A. B. Retik.** 1997. Continent urinary diversion: the Children's Hospital experience. J. Urol. **157:**1394–1399.
15. **Karkkainen, P., and M. Salaspuro.** 1991. Serum and urinary β-hexosaminidase as markers of heavy drinking. Alcohol Alcohol. **25:**365–369.
16. **Kok, D. J., J. Poindexter, and C. Y. C. Pak.** 1993. Calculation of titratable acidity from urinary stone risk factors. Kidney Int. **44:**120–126.
17. **Korn, A., Z. Rajabi, B. Wassum, W. Ruiner, and K. Nixdorff.** 1995. Enhancement of uptake of lipopolysaccharide in macrophages by the major outer membrane protein OmpA of gram-negative bacteria. Infect. Immun. **63:** 2697–2705.
18. **Leite, A. Z., A. M. Sipahi, A. O. Damiao, A. M. Coelho, A. T. Garcez, M. C. Machado, C. A. Buchpiguel, F. P. Lopasso, M. L. Lordello, C. L. Agostinho, and A. A. Laudanna.** 2001. Protective effect of metronidazole on uncoupling mitochondrial oxidative phosphorylation induced by NSAID: a new mechanism. Gut **48:**163–167.
19. **Li, D., M. Gallup, N. Fan, D. E. Szymkowski, and C. B. Basbaum.** 1998. Cloning of the amino-terminal and 5′-flanking region of the human MUC5AC mucin gene and transcriptional upregulation by bacterial exoproducts. J. Biol. Chem. **273:**6812–6820.
20. **Li, J. D., W. Feng, M. Gallup, J. H. Kim, J. Gum, Y. Kim, and C. Basbaum.**

1998. Activation of NF-κB via a Src-dependent Ras-MAPK-pp90^{rsk} pathway is required for *Pseudomonas aeruginosa*-induced mucin overproduction in epithelial cells. Proc. Natl. Acad. Sci. USA **95:**5718–5723.
21. **Luo, Y., J. D. Bond, and V. M. Ingram.** 1997. Compromised mitochondrial function leads to increased cytosolic calcium and to activation of MAP kinases. Proc. Natl. Acad. Sci. USA **94:**9705–9710.
22. **Mathoera, R. B., D. J. Kok, W. J. Visser, C. M. Verduin, and R. J. M. Nijman.** 2001. Cellular membrane associated mucins in artificial urine as mediators of crystal adhesion: an in vitro enterocystoplasty model. J. Urol. **166:**2329–2336.
23. **Mathoera, R. B., D. J. Kok, and R. J. M. Nijman.** 2000. Bladder calculi in augmentation cystoplasty in children. Urology **56:**482–487.
24. **Mobley, H. L. T., G. R. Chippendale, K. G. Swihart, and R. A. Welch.** 1991. Cytotoxicity of the HpmA hemolysin and urease of *Proteus mirabilis* and *Proteus vulgaris* against cultured human renal proximal tubular epithelial cells. Infect. Immun. **59:**2036–2042.
25. **Oelschlaeger, T. A., and B. D. Tall.** 1998. Uptake pathways of clinical isolates of *Proteus mirabilis* into human epithelial cell lines. Microb. Pathog. **21:**1–16.
26. **Schwartz, B. F., and M. L. Stoller.** 2000. The vesical calculus. Urol. Clin. N. Am. **27:**333–346.
27. **Shikhman, A. R., D. C. Brinson, and M. Lotz.** 2000. Profile of glycosaminoglycan-degrading glycosidases and glycoside sulfatases secreted by human articular chondrocytes in homeostasis and inflammation. Arthritis Rheum. **43:**1307–1314.
28. **Skulachev, V. P.** 1998. Cytochrome *c* in the apoptotic and antioxidant cascades. FEBS Lett. **423:**275–280.
29. **Tytgat, K. M., L. W. Klomp, F. J. Bovelander, F. J. Opdam, A. Van der Wurff, A. W. Einerhand, H. A. Buller, G. J. Strous, and J. Dekker.** 1995. Preparation of anti-mucin polypeptide antisera to study mucin biosynthesis. Anal. Biochem. **226:**331–341.
30. **Van Klinken, J. W., A. W. C. Einerhand, H. A. Büller, and J. Dekker.** 1998. Strategic biochemical analysis of mucins. Anal. Biochem. **265:**103–116.
31. **Vishwanath, S., R. Ramphal, C. M. Guay, D. DesJardins, and G. B. Pier.** 1988. Respiratory mucin inhibition of the opsonophagocytic killing of *Pseudomonas aeruginosa*. Infect. Immun. **56:**2218–2222.
32. **Waters, S. L., J. K. Wong, and R. G. Schnellmann.** 1997. Depletion of endoplasmic reticulum calcium stores protects against hypoxia- and mitochondrial inhibitor-induced cellular injury and death. Biochem. Biophys. Res. Commun. **240:**57–60.
33. **Wells, C. L., R. P. Jechorek, K. M. Kinneberg, S. M. Debol, and S. L. Erlandsen.** 1999. The isoflavone genistein inhibits internalization of enteric bacteria by cultured Caco-2 and HT-29 enterocytes. J. Nutr. **129:**634–640.
34. **Wells, C. L., E. M. van de Westerlo, R. P. Jechorek, and S. L. Erlandsen.** 1996. Intracellular survival of enteric bacteria in cultured human enterocytes. Shock **6:**27–34.

Editor: B. B. Finlay